Increasing opal productivity in the late Eocene Southern Ocean: Evidence for increased carbon export preceding the Eocene-Oligocene glaciation

Volkan Özen[1,2], Johan Renaudie[2], David B. Lazarus[2], Gabrielle Rodrigues de Faria[1,2]

[1]Freie Universität Berlin, Institute for Geological Sciences, Malteserstraße 74–100, 12249 Berlin, Germany
[2]Museum für Naturkunde, Leibniz Institute for Evolution and Biodiversity Science,
Invalidenstraße 43, 10115 Berlin, Germany

Correspondence to: Volkan Özen (volkan.oezen@fu-berlin.de)

Abstract. The Eocene/Oligocene Transition represents a period of profound changes in diatom productivity and evolutionary history within the Cenozoic era. Unraveling how these changes correlate with climatic shifts during this transition is crucial for understanding the potential role of diatoms in the cooling trends observed at the Eocene/Oligocene boundary (~33.9 Ma). Current research predominantly relies on bulk opal accumulation measurements to assess productivity dynamics, which fails to distinguish the contribution of different biosiliceous (e.g., diatom versus radiolarian) plankton to total biogenic silica productivity. Furthermore, despite the fundamental role of community composition and diversity in diatom productivity and carbon sequestration, these factors are often not incorporated in existing studies focusing on the late Paleogene diatom productivity. The main objective of our work is to explore the potential roles of diatom communities in the late Eocene climatic changes by focusing on diatom- and radiolarian-specific productivity across multiple Southern Ocean sites, rather than bulk opal measurements, and by incorporating total diatom abundance into the analysis of diatom diversity evolution throughout the Eocene/Oligocene transition. By quantifying diatom and radiolarian abundances across four Southern Ocean sites in the Atlantic and Indian Ocean sectors, and analyzing diatom productivity through recent reconstructions of diatom diversity from approximately 40-30 Ma interval, our findings reveal a significant increase in diatom abundance coupled with notable shifts in community diversity. These changes suggest a potential ecological shift, likely associated with the development of stronger circum-Antarctic currents in the late Eocene. Such shifts could have influenced the efficiency of the biological carbon pump by enhancing organic carbon export to the deep ocean and thus potentially contributing to reduced atmospheric CO_2 levels. While our findings indicate that the expansion of diatoms may have been a part of the mechanisms underlying the late Eocene cooling, they also highlight the importance of integrating diatom diversity and community evolution into diatom productivity research. Furthermore, our results offer valuable insights into the complex relationship between diatom abundance and diversity in the geological record, reflecting the intricate interplay of environmental and climatic factors.

1 Introduction

The Eocene/Oligocene boundary (E/O, ~33.9 Ma) marks the end of the Cenozoic Hothouse with high-latitude surface ocean cooling and an abrupt 1.5 per mil increase in global benthic $\delta^{18}O$ values (Shackleton and Kennett, 1975; Zachos et al., 1996, 2001; Coxall et al., 2005; Zachos and Kump, 2005; Coxall and Pearson, 2007; Liu et al., 2009; Westerhold et al., 2020; Hutchinson et al., 2021). It corresponds to the largest cooling shift of the late Paleogene gradual cooling trend and the abrupt emplacement/expansion of the Antarctic ice sheet (Lear et al., 2008). Despite the extensive research, the underlying mechanisms are under dispute. The discussions on the possible mechanisms have revolved around three main domains (1) gradual thermal isolation of Antarctica with the development of the Antarctic Circumpolar Current (ACC) initiated by the deepening of the Southern Ocean (here and after SO) gateways (Kennett, 1977; Barker, 2001), (2) the threshold response of the Earth climate to the atmospheric CO_2 decrease in the late Paleogene (DeConto and Pollard, 2003; Ladant et al., 2014), and (3) the evolution of the west Antarctic rift system, which might have significantly modulated ice-sheet volume and climate feedbacks (Wilson and Luyendyk, 2009; Wilson et al., 2013).

These mechanisms are possibly interlinked; oceanographic change, CO_2 drawdown, and tectonic reorganization of Antarctic topography are supported and extensively discussed by proxy records and model results (e.g., Scher and Martin, 2006; Ladant et al., 2014; Elsworth et al., 2017; Paxman et al., 2019; Toumoulin et al., 2020; Hutchinson et al., 2021; Lauretano et al., 2021; Klages et al., 2024). Within this broader framework, several studies have suggested that increased SO productivity may have contributed to CO_2 decline by linking changes in circulation to export productivity and carbon sequestration (e.g., Diester-Haass and Zahn, 1996; Salamy and Zachos, 1999; Schumacher and Lazarus, 2004; Egan et al., 2013; Rodrigues de Faria et al., 2024). Although the timing and characteristics of this productivity shift remain debated (Renaudie, 2016; Wade et al., 2020; Bryłka et al., 2024,; Rodrigues De Faria et al., 2024), it was likely a piece of the broader mechanistic mosaic underlying the E/O transition and Antarctic glaciation. Diatoms and radiolarians, as major siliceous plankton groups, are pivotal to these discussions, both as contributors to export production and as proxies for changing nutrient supply and ocean circulation. Their fossil records suggest significant reorganization across the late Eocene to early Oligocene interval (see Section 1.2).

1.1 Opal as a paleoproductivity proxy

Biogenic silica deposition in modern oceans reflects surface ocean productivity, a pattern observed consistently across diverse regions from the equatorial to high-latitude Pacific and Atlantic Oceans (Baldauf and Barron, 1990; Barron et al., 2015). Biogenic silica has higher preservation potential than organic carbon (Tréguer et al., 1995; Ragueneau et al., 2000 and references therein), signifying the potential of biogenic silica deposition in tracking the changing paleoproductivity trends throughout the Cenozoic. However, this proxy is complicated by variability in silica dissolution and preservation, as well as the decoupling of the silica-carbon relationship from surface waters to sediments (Ragueneau et al., 2000). The

factors influencing silica dissolution and preservation are not fully constrained and are expected to vary significantly under different oceanographic and climatic conditions throughout the Cenozoic (Ragueneau et al., 2000; Westacott et al., 2021). Although the links between the opal depositionand productivity dynamics are complex, it has been shown that the secular trend of opal deposition is closely related with the global oceanographic and climatic changes (Cortese et al., 2004).

70 Additionally, the evolutionary history of biosiliceous plankton underlying opal deposition during the Cenozoic is a critical but often overlooked aspect in paleoproductivity interpretations based on opal accumulation. Most available data are based on bulk opal measurements, which can obscure the contributions of different biosiliceous plankton groups, such as radiolarians (another extremely important siliceous plankton) and marine diatoms. Assessing the relative contributions of different biosiliceous plankton groups to opal sedimentation is essential for accurate paleoproductivity reconstructions

75 (Ragueneau et al., 2000, 2006).

1.2 Prior opal records and the role of diatom diversity in Southern Ocean productivity

Evidence from the SO suggests that productivity in the region increased during the late Eocene, with the first notable shifts occurring around 38–37 Ma (Diester-Haass and Zahn, 1996; Schumacher and Lazarus, 2004; Villa et al., 2014; Rodrigues de Faria et al., 2024). The rise in opal deposition during the late Eocene and at the E/O (Salamy and Zachos, 1999; Diekmann et

80 al., 2004; Anderson and Delaney, 2005; Bryłka et al., 2024), has been linked to the growing dominance of diatoms in open ocean settings. Given the central role of modern diatoms in carbon export through the biological carbon pump (e.g., Tréguer et al., 2018), these observations have drawn attention to a possible link between increased diatom productivity and atmospheric CO_2 decline at the E/O (Salamy and Zachos, 1999; Scher and Martin, 2006; Rabosky and Sorhannus, 2009; Egan et al., 2013; Renaudie, 2016). However, utilizing the opal deposition history to elucidate the diatom productivity across

85 the end-Eocene remains challenging because the data so far is based on bulk opal measurements which do not allow to assess the relative contribution of diatoms and other siliceous plankton, especially radiolarians. Although diatoms dominate opal sedimentation in modern oceans, radiolarians were more common in the early Paleogene, and the shift to diatom dominance occurred during a poorly constrained interval in the mid to late Paleogene (Renaudie, 2016).

90 The role of diatom diversity in driving productivity is also poorly constrained and often overlooked in paleoproductivity studies. Most reconstructions addressing late Paleogene opal deposition do not distinguish among siliceous groups and remain agnostic to the species diversity underlying the opal signal (Salamy and Zachos, 1999; Diekmann et al., 2004; Anderson and Delaney, 2005; Plancq et al., 2014). Yet in modern ecosystems, diverse plankton communities are associated with higher biomass production, carbon export, and greater ecological stability (Tréguer et al., 2018; Virta et al., 2019;

95 Hatton et al., 2024). A positive, often unimodal, relationship between diversity and productivity has been documented across many taxa, particularly groups of plants on global scales (Mittelbach et al., 2001). However, in paleoceanography, the link between diatom diversity and abundance/productivity is not well understood. Diatom diversity has at times been used as a proxy for abundance (Lazarus et al., 2014), tough molecular data complicate this assumption by showing comparable

diversity values in both eutrophic and oligotrophic settings (Malviya et al., 2016). These findings point to the need to re-evaluate the diversity-productivity relationship in fossil plankton communities using direct, paired observations.

In this study, we aim to improve constraints on SO diatom productivity across the late Eocene–early Oligocene interval by distinguishing the relative contributions of diatoms and radiolarians to total biogenic silica deposition. We present newly generated mass accumulation rate (MAR) data for both groups, based on the same sediment samples used in recent biological barium (bio-Ba) reconstructions (Rodrigues de Faria et al., 2024). By comparing these group-specific accumulation records with bulk opal and bio-Ba productivity estimates, we provide an independent assessment of siliceous plankton dynamics across the transition. Finally, we explore the relationship between diatom abundance and diversity to discuss the long-presumed link between diatom diversity and abundance.

2 Methods

2.1 Material

We analyzed diatom and radiolarian abundance data from samples collected from the following SO sites: Deep Sea Drilling Project (DSDP) Site 511 (Falkland Plateau, 51°00.28'S; 46°58.30'W) (sampled interval ~27–180 meter below sea floor (mbsf)), Ocean Drilling Project (ODP) Site 1090B (Agulhas Ridge, 42°54.8′S 8°53.9′E) (~188-335 mbsf), ODP Site 748B (Kerguelen Plateau, 58°26.45′S; 78°58.89′E) (~96–171 mbsf), and ODP Site 689D (Maud Rise, 64°31′S 3°6′E) (~104–132 mbsf) (Fig. 1). Our study examines 53 samples spanning the temporal interval from the late Eocene to the early Oligocene, approximately between 39 and 30 Ma, with site-specific coverage varying due to differences in sedimentation history at each site.

DSDP Site 511 (Falkland Plateau) and ODP Site 1090 (Agulhas Ridge) contain hiatuses in the earliest Oligocene, limiting the temporal coverage of these sites. At DSDP 511, our samples' temporal coverage is ~37.5–32.5 Ma. Similarly, at Site 1090, the sampled interval spans ~38–33 Ma, with a hiatus restricting samples from extending well into the Oligocene. In contrast, at ODP Site 689 (Maud Rise) and ODP Site 748 (Kerguelen Plateau), sedimentation is relatively continuous, providing a more complete record of the EOT (~36.5–30 Ma at Site 689; ~40–29 Ma at Site 748). All analyzed samples and corresponding measurements, including diatom and radiolarian abundance data, are detailed in the Supplementary Materials.
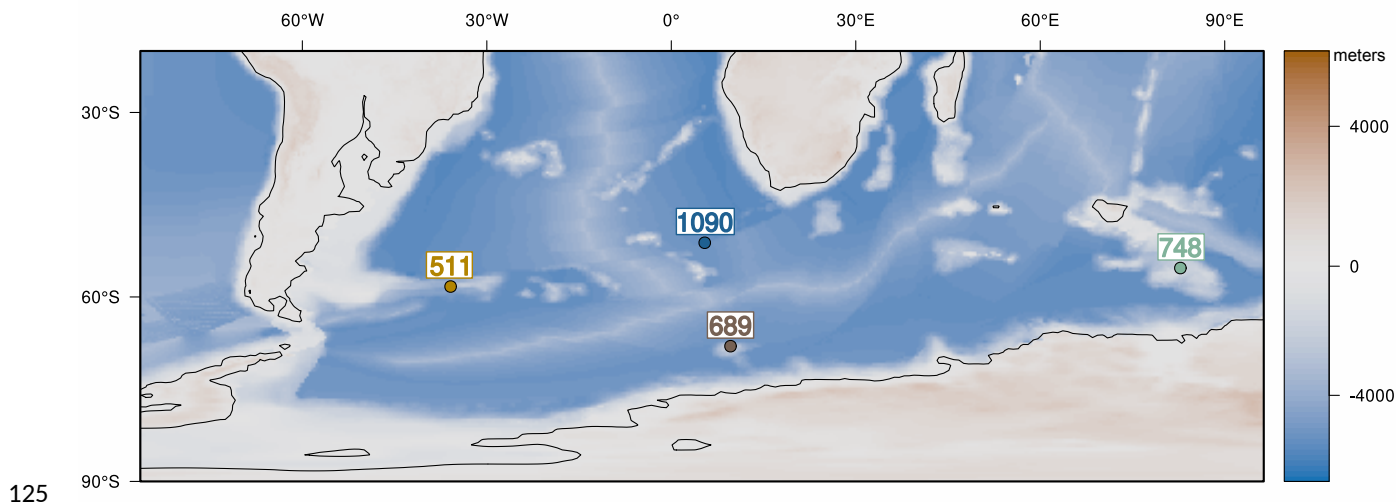
Figure 1: Locations of the studied Southern Ocean sites, shown on a late Eocene paleogeographic and paleobathymetric reconstruction (adapted from Straume et al. 2024). Estimated paleodepths at the E/O boundary: 2436 mbsl at DSDP Site 511; 2036 mbsl at ODP Hole 689D; 1270 mbsl at ODP Hole 748b and 3358 mbsl at ODP Hole 1090B (see Methods)

In the southern high latitudes, DSDP Site 511 and ODP Site 1090 are notable for being a major locus of biogenic silica deposition across the Eocene/Oligocene transition (e.g., Diekmann et al., 2004; Anderson and Delaney, 2005; Renaudie, 2016; Wade et al., 2020). While ODP Site 689D and 748B, in general, do not exhibit the same level of opal productivity, significant productivity changes have been documented at these sites across the E/O transition (e.g., Salamy and Zachos, 1999; Bryłka et al., 2024). These findings signify that these sites provide invaluable insights into the SO productivity in the areas proximal to the Antarctic continent. They provide essential insights into how opal productivity varies under different regional settings, offering a broader perspective on productivity changes across the SO.

A comprehensive overview of the updated age models used in this study for each Hole/Site is available in Rodrigues de Faria et al. (2024); see also Supplementary Text 1. The models can also be accessed via the Neptune Database (Renaudie et al., 2020, 2023). Paleobathymetry at each site at the E/O boundary was computed using those age models and each hole lithological decriptions from their corresponding Initial Reports (Shipboard Scientific Party 1983, 1988, 1989, 1999) using PyBacktrack (Müller et al. 2018). The files used as input for PyBackTrack can be found in the SOM, as well as its output.

2.1.1 Sample Preparation

Microscope slides for counting diatom and radiolarian abundances were prepared following a modified version of the methods described by Moore (1973) and Lazarus (1994) and sieved using a 10 μm sieve. About 0.5–1 gram sediment was treated with hydrogen peroxide (H_2O_2) and pentasodium triphosphate ($Na_5P_3O_{10}$) over heat, followed by treatment with hydrochloric acid (HCl). The resulting solution was then sieved through a 10 μm sieve. A controlled amount of the residues

was then gently settled over three coverslips at the bottom of a beaker. This approach ensures the material settles randomly across the coverslips, minimizing potential biases might arise during the enumeration phase (for details, see Lazarus, 1994).

2.2 Diatom and radiolarian absolute abundance and accumulation rates

150 Absolute abundances **(ab)** for diatoms and radiolarians were calculated by counting specimens on a known area of slides, following the equation below:

$$ab = N \times (Ab/Am) \times (Vp/Vu) \times 1/w \tag{1}$$

155 with N is being the number of specimens counted, Ab the area of used beaker (6079 mm2), Am the area measured in mm^2, Vp the volume of residue prepared in mL, Vu the volume used in mL and w the weight of the dry sediment in gram.

Accumulation rates of diatoms and radiolarians were calculated by multiplying abundance values with the shipboard measured dry bulk densities and the linear sedimentation rates (LSR). The LSR values applied are based on updated age
160 models for the targeted sites.

2.3 Diatom abundance and diversity

Our study also examines the relationship between diatom diversity and total diatom abundance, which is essential for understanding the influence of diversity on overall community productivity in diatoms. Rather than relying on bulk opal accumulation rates, which do not distinguish the relative contribution of different siliceous groups like radiolarians, we
165 focused on diatom-specific abundance values. This approach provides a clearer understanding of the relationship between diversity and abundance within diatom communities.

To explore these interactions, we compared recent diatom diversity reconstructions (Özen et al., subm.) with diatom abundance data obtained in this study across the E/O transition. This approach allowed us to directly examine how variations
170 in diatom diversity correspond to changes in abundance and to explore the potential implications of these interactions for overall diatom productivity. In our comparisons, by focusing on diatom abundances per gram of sediment, we aimed to minimize potential biases associated with accumulation rates, which can be affected by uncertainties in age models. This approach ensures a more accurate representation of the abundance-diversity relationship, offering valuable insights into the ecological and environmental factors that influenced diatom productivity during the E/O transition.

3 Results

Our diatom MARs reveal a clear latitudinal organization in the late Eocene SO.This is expected, as diatoms are a major contributor of biogenic sedimentation at sub-Antarctic sites, DSDP Site 511 (Falkland Plateau) and ODP site 1090 (Agulhas Ridge), where biogenic silica is the main sedimentary component across the study interval (Renaudie, 2016; Wade et al., 2020; see Fig. S1).

In the sub-Antarctic Atlantic,ODP Site 1090 diatom MAR increased from ~38 Ma onward, peaking around 36.8 Ma, closely matching previously published bulk opal MARs (Diekmann et al., 2004; Anderson and Delaney, 2005, see Fig. 2d and 2e). Site 1090 had an average diatom MAR of 1.26×10^7 frustules/cm^2/kyr (with standard deviation (std dev.) 9.48×10^6, ranging from 5.88×10^5 to 3.26×10^7. The total number of samples (N) = 15). At DSDP Site 511, diatom MARs gradually rose throughout the late Eocene, peaking near 33.4 Ma (1.76×10^8, see Fig. 2e), with notably higher accumulation rates (mean = $5.73 \times 10^7 \pm 4.97 \times 10^7$; range: $1.65 \times 10^7 - 1.77 \times 10^8$, N = 9). The overall diatom MAR trends at this site align well with recent bulk opal accumulation rates (Bryłka et al., 2024, Fig. 2d). Fig. 3a shows the distributional characteristics of diatom MARs at both sites.
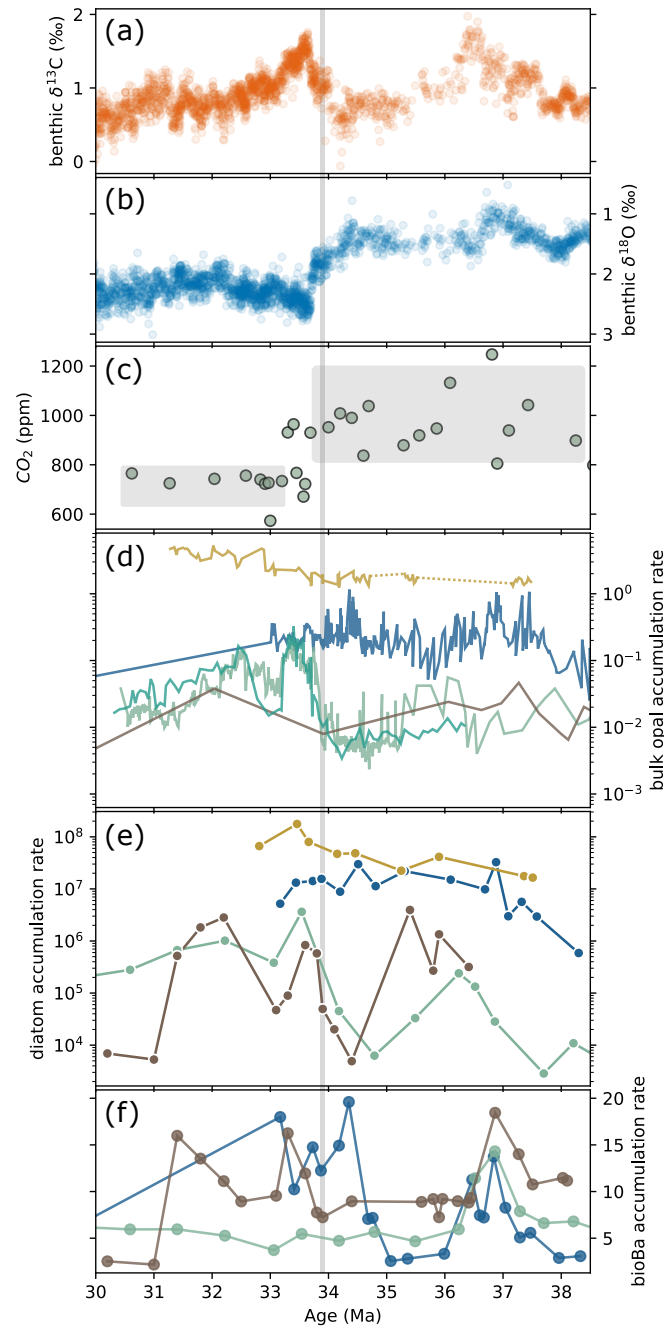
Figure 2. (a) Global composite benthic foraminiferal $\delta^{13}C$ and (b) $\delta^{18}O$ records (from Westerhold et al., 2020). (c) CO_2 compilation (from Zhang et al., 2013; Anagnostou et al., 2020). (d) Bulk opal accumulation rates (gr cm^{-2} kyr^{-1}, solid lines) from DSDP 511 (yellow, Bryłka et al., 2024), ODP 1090 (blue, Diekmann et al., 2004; Anderson and Delaney 2005), Kerguelen Plateau ODP Sites (light green, 744 and 738; dark green 748) (compiled from Ehrmann, 1991; Ehrmann and Mackensen, 1992; Salamy and Zachos, 1999, Bryłka et al., 2024), and ODP 689 (Faul and Delaney, 2010). (e) Diatom mass accumulation rates (MARs) (diatom cm^{-2} kyr^{-1}; scatter points with solid lines; this study) and (f) biogenic barium (bioBa) accumulation rates (μmol cm^{-2} kyr^{-1}) from ODP Sites 1090, 689, and 748 (from Rodrigues de Faria et al., 2024).

Antarctic sites showed lower and more variable diatom MARs (Fig. 2e and 3a). At ODP Site 689 (Maud Rise), diatom MAR

200   exhibited prominent peaks (within the temporal precision of our data) at ~35.5 Ma, 33.6 Ma, and 32.3 Ma, with an average

value of 7.92×10^5 frustules/cm^2/kyr (std dev. is 1.16×10^6, range: $4.92 \times 10^3 – 3.94 \times 10^6$, N = 16; see Fig. 2e). At ODP Site

748 (Kerguelen Plateau), diatom and bulk opal MARs are in agreement after ~37.5 Ma, suggesting increasing diatom

contribution to the total opal productivity towards the E/O boundary. Mean diatom MAR at this site is 3.74×10^5, with

minimum and maximum values of 2.86×10^3 and 3.63×10^6, respectively (N = 18). At this site, it has been shown that across

205   the middle Eocene, other siliceous groups, ebridians and radiolarians, dominate the record (Witkowski et al., 2012).

Combined with our results, this suggest that diatom dominance in the Kerguelen Plateau region started in towards 37 Ma,

which is consistent with our sample surveys that there is a strong presence of ebridians in our samples preceding ~38 Ma

(See Supplementary Data 1). Moreover, our results show that, compared to the other sites, diatom MAR at ODP Site 748B

changed substantially between Eocene and Oligocene (Fig. 3a), with a mean of 4.8×10^4 frustules/cm^2/kyr in the Eocene

210   and 1.03 in the Oligocene.
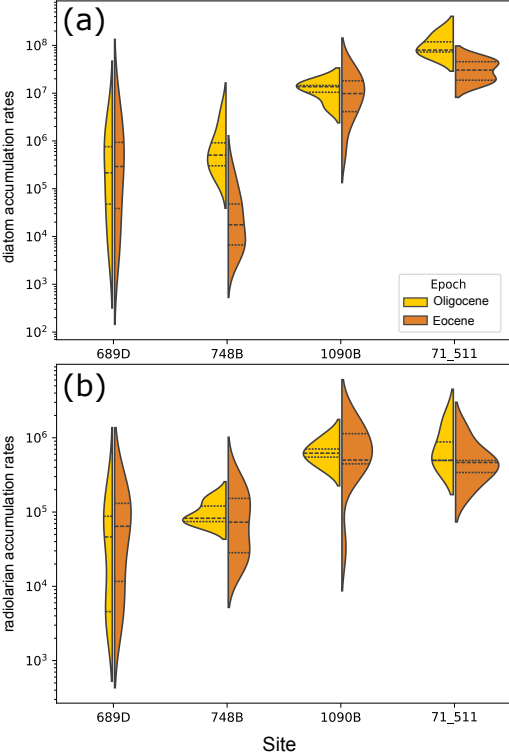
Figure 3. Distribution of MARs (specimen cm^{-2} kyr^{-1}; in log scale) for (a) diatoms and (b) radiolarians at each studied site (x-axis). Eocene and Oligocene samples are shown separately (see legend). Lines within each distribution indicate the quartiles, marking
215   **the median, the 25th and 75th percentiles.**

Our diatom MARs, combined with published bulk opal MAR records, reveal two distinct intervals during the EOT, 36.5–35.5 Ma and 34–33 Ma, when opal productivity at Antarctic sites (ODP 689 and 748) sharply increased, approaching sub-Antarctic Atlantic levels (Fig. 2d and 2e). Although sub-Antarctic sites (DSDP 511 and ODP 1090) maintained consistently higher opal productivity throughout the EOT, Antarctic sites experienced transient but significant increase in diatom MARs during these intervals, bringing opal flux levels closer to those observed at sub-Antarctic sites.

These intervals, of Antarctic and sub-Antarctic diatom MAR convergences, unfolded under distinct climatic conditions. The first (~36.5–35.5 Ma) interval broadly aligns with the late Eocene warming event, which has been documented at multiple high-latitude SO sites (ODP Site 689 (Maud Rise); ODP Sites 738, 744, 748 (Kerguelen Plateau); DSDP Site 277 (Diester-Haass and Zahn, 1996; Bohaty and Zachos, 2003; Villa et al., 2008, 2014; Pascher et al., 2015). In contrast, the later interval (~34–33 Ma) broadly concomitant with a sharp increase in global foraminiferal $\delta^{18}O$ in the earliest Oligocene, signalling substantial cooling and the onset of permanent Antarctic glaciation (Fig. 2b and 2d). Although diatom MAR at Antarctic sites temporarily approached sub-Antarctic levels during both intervals, the associated environmental conditions differed markedly.

Radiolarian MAR patterns are broadly in agreement with diatom MARs acro ss the E/O transition, derived from the same samples (Fig 4c). At ODP Site 1090, radiolarian MARs showed two prominent peaks at ~37 and 34.5 Ma. The mean accumulation rate at this site is 7.43×10^5 radiolaria/cm²/kyr ($\pm 4.56 \times 10^5$, range: 3.29×10^4–1.60×10^6). At DSDP Site 511, MAR values remained relatively stable throughout the late Eocene, exhibiting significant increases towards and after the E/O boundary, at approximately 34 Ma and 33.5 Ma (mean = $6.34 \times 10^5 \pm 4.53 \times 10^5$, range: 1.79×10^5–1.56×10^6).

At ODP Site 748, radiolarian MAR peaked notably at ~36.5 Ma, followed by a substantial decline, and recovered to pre-E/O levels only around 30.5 Ma (mean = $1.01 \times 10^5 \pm 7.61 \times 10^4$, range: 1.73×10^4–3.06×10^5). ODP Site 689 indicated two prominent peaks, between 36–35 Ma, and at ~31.5 Ma, with a lower average MAR of 6.49×10^4 ($\pm 6.20 \times 10^4$, range: 3.89×10^3–1.85×10^5). From ~35 Ma onward, radiolarian MAR differences between sub-Antarctic Atlantic (sites 1090 and 511) and Antarctic (sites 689 and 748) sites became more pronounced, reflecting an increasing contrast in accumulation rates during the latest Eocene – early Oligocene (Fig. 4c; see also Fig. S2).
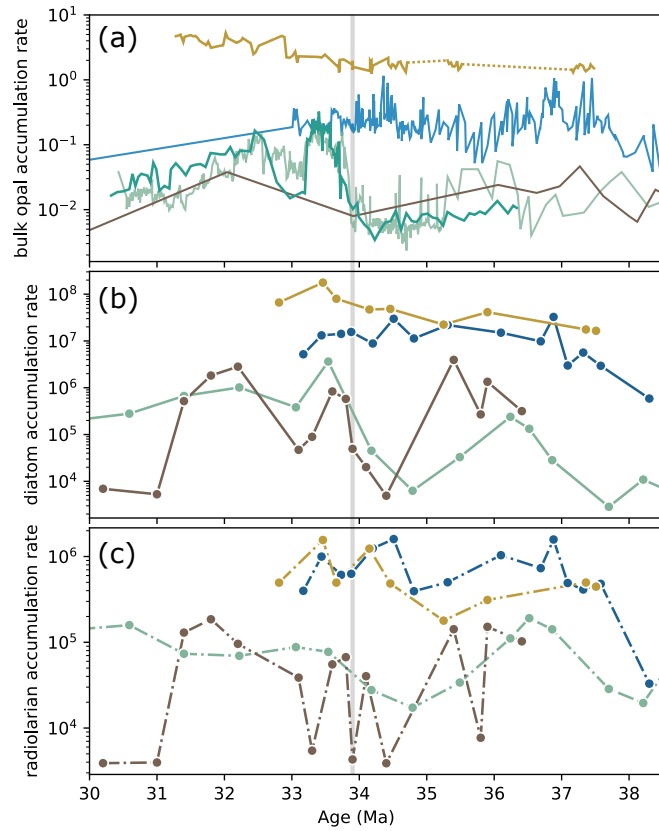
Figure 4. Comparison of (a) bulk opal, (b) diatom, and (c) radiolarian accumulation rates (specimen cm⁻² kyr⁻¹) at SO sites. Site colors are consistent across figures. Diatom and radiolarian data are from this study, while bulk opal accumulation rates (a; g cm⁻² kyr⁻¹, solid lines) are compiled from the following sources: DSDP 511 (yellow; Bryłka et al., 2024), ODP 1090 (blue; Diekmann et al., 2004; Anderson and Delaney, 2005), Kerguelen Plateau sites ODP 744 and 738 (light green) and ODP 748 (dark green) (Ehrmann, 1991; Ehrmann and Mackensen, 1992; Salamy and Zachos, 1999; Bryłka et al., 2024), and ODP 689 (Faul and Delaney, 2010).

3.1 Correlations between diatom diversity and abundance

Diatom abundance and diversity showed varied correlations among sites across the late Eocene – early Oligocene interval (Fig. S3). At DSDP Site 511, exhibiting the highest species diversity, diatom abundance and diversity were in great agreement across the E/O transition (Fig. 4c; see also Fig. S3). At ODP Site 1090, diatom abundance and diversity were generally synchronous, except between approximately 37 and 34.5 Ma, during which diversity values stayed relatively low and constant while abundance values showed the highest values. Moreover, the pronounced peaks in diatom abundance around 36.8 and 34.5 Ma did not correspond with similar increase or trend shift in diatom diversity (Fig. 5d). In contrast, at ODP Sites 689 and 748, diatom diversity and abundance values were in agreement (Fig. 5b and 5e ; Fig. S3). At ODP Site 748, there was a substantial increase in both bulk opal (Bryłka et al., 2024, Fig. 5a) and diatom abundance, reaching values

similar to those seen at sun-Antarctic Atlantic sites ODP 1090 and DSDP 511. However, diversity values remained
265 significantly lower compared to those documented at the sub-Antarctic Atlantic sites (Fig. 5e).
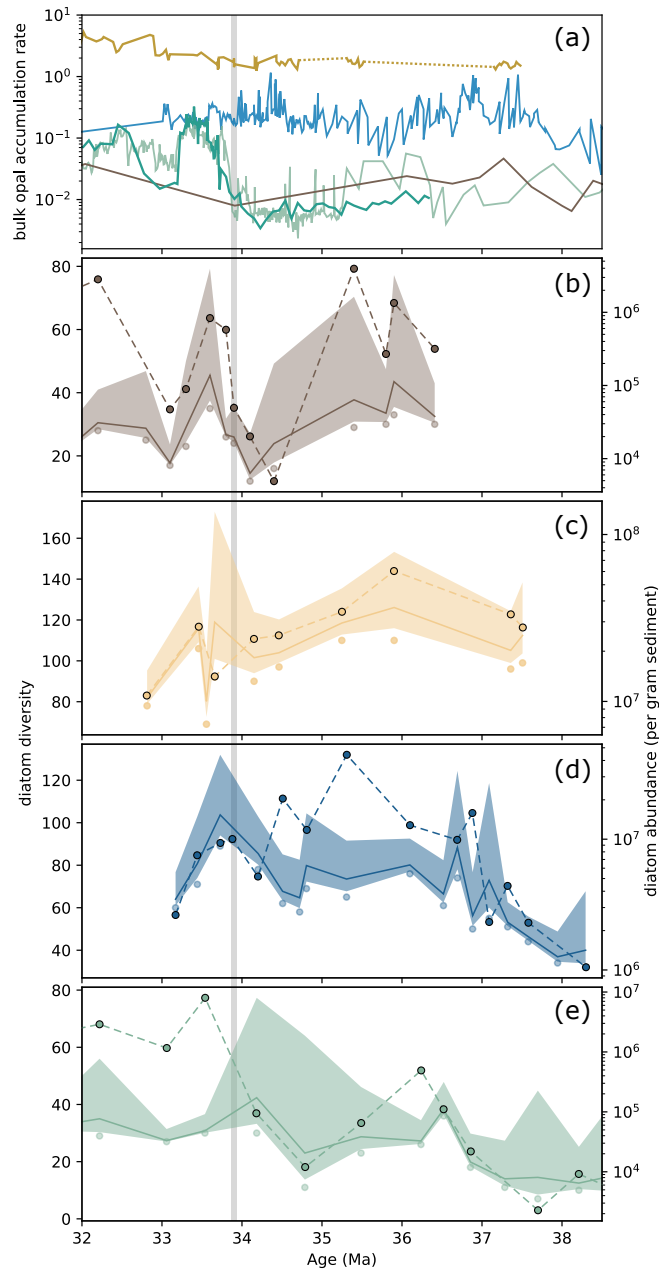
Figure 5. Comparison of bulk opal accumulation rates (gr cm⁻² kyr⁻¹) with diatom diversity (number of species) and abundance. (a)
270 **from DSDP 511 (yellow, Bryłka et al., 2024), ODP 1090 (blue, Diekmann et al., 2004; Anderson and Delaney, 2005), Kerguelen**
Plateau ODP Sites (light green, 744 and 738; dark green 748) (compiled from Ehrmann 1991; Ehrmann and Mackensen 1992;

Salamy and Zachos, 1999; Bryłka et al., 2024), and ODP 689 (brown, Faul and Delaney, 2010) (b-e) Diatom diversity (scatter points) with Chao1 diversity estimates (solid line, 95% confidence envelope) (Özen et al., subm.) and diatom abundance per gram sediment (scatter points, dashed lines).

4 Discussion

4.1 Diatom and radiolarian productivity and opal record across the middle-to-late Eocene transition (~36–38 Ma)

Although the timing and mode of opal productivity (that is, the relative contribution of diatoms and radiolarians, the underlying diatom diversity, and whether the flux is pulsed or gradual) differ among sites, our results suggest a substantial reorganization of SO diatom and radiolarian productivity between ~38 and 36 Ma. In the sub-Antarctic Atlantic, bulk opal at ODP Site 1090 shows a gradual increase 38 Ma onwards, intensifying by ~37 Ma (Diekmann et al., 2004; Anderson and Delaney, 2005). Our diatom MARs closely follow this trend, suggesting growing diatom dominance in the region. This shift was not confined to a single site or proxy but occurred across multiple sectors: radiolarian communities in the South Pacific reorganized (Pascher et al., 2015), and in the Indian Ocean sector both bulk opal and diatom MARs rise between ~38-36 Ma (Fig. 2d-e, ODP 748 and 744), in parallel with evidence for increasing eutrophic conditions from calcareous nannofossil (Villa et al., 2014, see Fig. S4), confirming that the diatom signal reflects a real productivity shift.

In the Atlantic sector, benthic foraminiferal accumulation rates (Diester-Haass and Zahn, 1996, see Fig. S5) and radiolarian communities (Funakawa and Nishi, 2008) record this shift in productivity and environmental conditions. Bio-Ba records from ODP Sites 1090, 689, and 748 (Rodrigues de Faria et al., 2024) document a ~37 Ma export productivity peak that is synchronous with the diatom MAR rise at ODP Site 1090 but leads peaks at Antarctic-adjacent sites (ODP 689, 748) by ~0.5–1 Myr (Fig. 2e). This offset does not reflect differences in age models, as identical samples and age models were used in both datasets, and likely reflects regional environmental controls during middle-to-late Eocene, including latitudinal differences in sea-surface temperature (e.g., Douglas et al., 2014; Sauermilch et al., 2021), variations in nutrient distribution, and circulation patterns influenced by still-shallow SO gateways (e.g, Sauermilch et al., 2021; Rodrigues de Faria et al., 2024).

What does this productivity reorganization across the middle-to-late Eocene transition (~38–36 Ma) signify? It encompasses a suspected ephemeral East Antarctic glaciation, namely Priabonian Oxygen Maximum (PrOM, ~37 Ma; Scher et al., 2014). This event is marked by a sharp negative Neodymium (Nd) excursion within a broader late Eocene positive trend (Scher and Martin, 2006; Scher et al., 2014; Wright et al., 2018). Previous studies link PrOM cooling to productivity shifts across SO sectors (e.g., Villa et al., 2014; Pascher et al., 2015; Rodrigues de Faria et al., 2024) through mechanisms involving transient intensification and organization of a proto-ACC that enhanced frontal upwelling and nutrient delivery (e.g., Rodrigues de Faria et al., 2024). This interpretation is consistent with modelling results suggesting that even a shallow opening of the Drake Passage, which likely during the late middle-Eocene (Scher and Martin, 2004; 2006), could have reorganized ocean

flow and promoted proto-ACC formation (Toumoulin et al., 2020). A comparable mechanism operates in the modern SO, where the strength of the latitudinal temperature gradient controls westerly wind intensity, which governs ACC transport and the intensity of wind-driven upwelling (R. Rintoul et al., 2001). In parallel, PrOM cooling, in line with southern high-latitude SST compilations (O'Brian et al., 2020), would have steepened the temperature gradient, intensified the westerlies that drive proto-ACC, and increased Ekman divergence, delivering nutrient-rich waters to the surface ocean. Silicon isotope data further support this scenario, indicating increased diatom silicic acid utilization during this interval and pointing to enhanced silicic acid supply to surface ocean via intensified upwelling (Egan et al., 2013). Consistent with this, although site level responses vary, diatom and radiolarian accumulation rates between 38 and 36 Ma show positive covariation at Agulhas Ridge and the Kerguelen Plateau. This pattern is more consistent with a shared physical driver, enhanced upwelling and nutrient supply, than with competitive replacement under constant nutrient conditions.

We note that, in addition to diatoms and radiolarians, other sources of biogenic silica, such as sponge spicules, silicoflagellates and ebridians, can also contribute to bulk opal, which may complicate direct comparisons with group-specific records. In our samples, these groups are not a significant component. Our focus therefore remains on diatoms and radiolarians to assess how their contributions changed through time within the broader biogenic silica pool, rather than attempting a one-to-one correspondence with bulk opal records.

Viewed in broader context, these productivity changes in diatom and radiolarian record and community composition across the middle-to-late Eocene transition (~36–38 Ma) (e.g., Pascher et al., 2015; Özen et al., subm.) are interpreted here as a response to increasing SO circulation and associated enhancements in nutrient distribution and upwelling. At the same time, this transition marks the onset of global rise in diatom abundance and diversity (Renaudie et al., 2016), and in our records diatom MARs show a net increase at all sites except ODP 689 during the subsequent interval, pointing to a basin-wide reorganization of diatom export. Indeed, comparable opal productivity surges during ~38–36 Ma are recorded in the equatorial Atlantic (Nilsen et al., 2003; Fig. S6) and northern Atlantic (Witkowski et al., 2021), suggesting that reorganization had a broad geographic reach and may reflect the strengthening of a cross-latitudinal circulation system akin to the modern Atlantic Meridional Ocean Circulation (AMOC). Indeed, it has been proposed that ~38 Ma onwards this circulation started to strengthen under the effect of increasing circum-Antarctic circulation, the proto-ACC, which is an integral part of the cross-latitudinal circulation across the Atlantic (Borrelli et al., 2014). This aligns with our diatom accumulation rates, which show a substantial reorganization 38 Ma onwards, aligning with earlier paleoproductivity reconstructions suggesting a substantial productivity increase across the SO sites between 36–38 Ma (e.g., Diester-Haass and Zahn, 1996; Pascher et al., 2015; Rodrigues de Faria et al., 2024). Although the precise timing and sequence of SO gateway opening and the development of circum-Antarctic circulation patterns remain debated (Diester-Haass and Zahn, 1996; Mackensen, 2004; Stickley et al., 2004; Scher and Martin, 2006; Livermore et al., 2007; Barker et al., 2007; Hodel et al., 2021; Evangelinos et al., 2024), the balance of evidence suggests a late Eocene strengthening **of circum-Antarctic**

circulation, possibly during the middle-to-late-Eocene transition, that set the stage for a large-scale reorganization of SO
340 productivity and the growing dominance of diatoms.

4.2 Opal pulse across the E/O boundary

Two overarching patterns characterize SO productivity across the E/O boundary (~35.5–32 Ma): (1) strong regional heterogeneity (see Bryłka et al., 2024; Rodrigues De Faria et al., 2024), and (2) distinct latitudinal responses. During the latest Eocene, diatom and radiolarian MARs diverge between sub-Antarctic (DSDP 511; ODP 1090) and Antarctic sites
345 (ODP 689; ODP 748). At the Antarctic sites, both groups decline (Fig 4b-c), consistent with low bulk-opal values on the Kerguelen Plateau and bio-Ba signals (Fig. 2d and 2f). In contrast, sub-Antarctic records show high latest-Eocene productivity: bulk opal, diatom MARs, and bio-Ba peak near ~34.5 Ma, especially at Agulhas Ridge (ODP 1090), while the Falkland Plateau (DSDP 511) maintains high diatom productivity (see Fig 2d-e).

350 Latitudinal divergence between sub-Antarctic and Antarctic sites strengthens from ~35.5 Ma onward (Fig. 4a-c; Fig. S2). This divergence is also evident in radiolarian productivity: before ~35.5 Ma, radiolarian MARs co-vary between the two regions, but from 35.5 Ma onward they diverge, signalling a change in biogeography and productivity. Indeed, radiolarian endemism in the southern high latitudes rises from ~35.5 Ma (Lazarus et al., 2008), consistent with greater regional isolation or reorganization of water masses. Tectonic reconstructions point to further Tasmanian Gateway (TG) deepening at about the
355 same time (Stickley et al., 2004), although Nd-isotope data imply that fully developed deep throughflow likely did not establish until the Neogene (Evangelinos et al., 2022). A step-like increase in the negative Ce anomaly at ~35.5 Ma indicates increased oxygenation of thermocline and bottom waters in the SW Pacific (Hodel et al., 2022), and the authors link this change to TG tectonic evolution and enhanced vertical mixing. Against this background circulation change, the Kerguelen Plateau region records a gradual ecological transition from a radiolarian-dominated to a diatom-dominated phase (Fig S7).
360 This shift occurs while overall opal flux remains low in the Antarctic-adjacent sites, pointing to altered competitive balance between siliceous plankton rather than a simple increase in nutrient supply. Broader confirmation of circulation reorganization comes from dinocyst biogeography and sedimentological evidence, which record stronger SO circulation and surface cooling from ~35.7 Ma (Houben et al., 2019).

365 Taken together, these lines of evidence indicate that circum-Antarctic circulation, which had already begun to strengthen across the middle-to-late Eocene transition, underwent further intensification from ~35.5 Ma. We interpret this reinforcement of circulation and vertical mixing as the main driver of the growing divergence between sub-Antarctic and Antarctic sites. Model simulations are consistent with this view: experiments with late-Eocene boundary conditions show that progressive gateway deepening enhanced eastward circumpolar flow, reorganized upper-ocean circulation, and shifted deep-convection
370 zones northward toward ~40 ºS, encapsulated the Agulhas Ridge region (Toumoulin et al., 2020). This circulation shift has indeed been linked to substantial export productivity at ODP Site 1090 in the latest Eocene (Rodrigues De Faria et al., 2024;

Fig. 2f), which possibly also underlies the opal productivity burst and overall high diatom productivity we observe at this site (Fig. 2d-e). At the same time, this northward shift of deep-convection would have reduced circulation strength in Antarctic-proximal sectors, particularly the Weddel region (see Toumoulin et al., 2020), which in turn would have reduced upwelling, nutrient supply, and export production (Rodrigues De Faria et al., 2024). The combined effect of a further strengthening proto-ACC and a weakened Antarctic circulation system offers a plausible mechanism for the sustained decline in diatom and radiolarian productivity at Antarctic sites from ~35.5 Ma to the E/O boundary.

In Antarctic-adjacent sites, the latest Eocene low-productivity regime shifts at the E/O boundary. Diatom MARs rise sharply, closely matching bulk-opal accumulation (Fig 2d) and coinciding with the largest increase in global $\delta^{18}O$ values (Fig. 2b), suggesting a link between the East Antarctic glaciation, cooling, and enhanced diatom productivity. Clay-assemblage studies suggest stronger physical weathering in the earliest Oligocene at Maud Rise (ODP 689) and the Kerguelen Plateau (ODP 748) (Robert et al., 2002). Such weathering likely increased silica input and fueled higher productivity in these regions. Consistently, the earliest-Oligocene Nd-isotope excursion in the Kerguelen Plateau, tied to glaciation and weathering (Scher et al., 2011), strongly correlates with opal flux (see Fig. S8), reinforcing the link between continental discharge and silica supply. In contrast, radiolarian productivity does not return to early late-Eocene levels (Fig. 4c). Instead, it remains low while diatoms increase strongly, suggesting that diatoms progressively gained dominance, likely reflecting their competitive advantage in utilizing the available silicic acid.

We note that geographically variable diatom flux across SO sites may not necessarily imply regionally inconsistent forcing. Sub-Antarctic sites supported diverse diatom communities (see Section 4.3) and already sustained high fluxes in the late Eocene, likely operating close to ecological carrying capacity, which may have muted the magnitude of their response. The biological basis for such a ceiling is well captured by the relationship between abundance and silicic acid in coastal upwelling zones: sedimentary diatom abundance increases as silicic acid concentrations rise until a threshold is reached, beyond which further silicic acid input yields little additional diatom accumulation (Abrantes et al., 2016). This diminishing return complicates efforts to trace a coherent sequence of diatom productivity and oceanographic reorganization across the SO, because increased silica supply via upwelling in already productivity sub-Antarctic regions, such as DSDP 511 and ODP 1090, may have altered community composition or frustule silicification rather than producing a proportional increase in diatom productivity and thus opal flux.

4.3 Diatom diversity and productivity: A cause/effect relation?

One of the defining features of SO opal productivity across the E/O transitions is its parallel with major changes in both diatom and radiolarian community composition (Funakawa and Nishi, 2008; Lazarus et al., 2008; Pascher et al., 2015; Özen et al., subm.). Under the influence of the dynamic climatic and oceanographic features of the SO, and within the limits **of** the fossil data resolution, it is a complex task tracking the exact ecological response dynamics of the biosiliceous plankton. The

changing diatom community composition and increasing diversity (Özen et al., subm.), is however expected to be positively associated with the range of functional traits within the community (Tréguer et al., 2018), and this to increasing efficiency in the nutrient utilization which is one of the operating terms for the biological carbon pump efficiency (Farmer et al., 2021).

The close relationship between observed diversity and diatom MARs and abundance, however, does not necessarily reflect a simple cause-effect link. Observed diversity could increase as a function of abundance through ecological interactions, or it could be an artefact of higher opal flux, better frustle preservation, and thus more morphologies recorded. Our findings suggest that while there is a notable correlation between diversity and abundance (see Fig. 5b-e), the relationship is not straightforward, reflecting a more intricate interplay between these two metrics. At ODP Site 748, for instance, diatom abundance rise sharply in the earliest Oligocene (Fig. 5e), yet diversity remains relatively low, barely reaching 30 species. This contrasts with observations at ODP Site 1090, where similar abundance values are associated with much higher diversity, suggesting that abundance alone does not drive diversity (Fig. 5d). Furthermore, at ODP 1090, a period of consistently high diatom abundance between 36.5 and 34.5 Ma corresponds to relatively low and stable diversity, indicating community stability rather than a direct abundance-diversity coupling. Notably, this interval at ODP Site 1090 is marked by the dominance of a specific diatom genus, *Pyxilla*, (Özen et al., subm.) which is likely contributed to the observed stability in diversity despite high overall abundance. Interestingly, in the second opal pulse at ODP 1090, diversity declines while abundance remains high, further illustrating that diversity and abundance need not covary, nor can diversity be reduced to a function of preservation alone.

On the other hand, data from DSDP Site 511 reveal a strong alignment between diatom abundance and diversity (Fig. 5c). This can be interpreted in an ecologic context, suggesting that the strength of the diversity-abundance relationship can vary considerably depending on the site-specific conditions, community composition, and the associated functional groups. Comparable patterns are seen in the modern ocean: metabarcoding surveys indicate that diatom diversity is not uniformly coupled to abundance but instead reflects the balance between a few dominant species and many rare ones, structured by regional circulation and ecological filtering (Malviya et al., 2016). This perspective reinforces the importance of incorporating biological and ecological dimensions into palaoproductivity studies on diatoms, in line with previous work emphasizing the role of community composition in maintaining ecosystem function and the efficiency of carbon export through diatomaceous pathways (Tréguer et al., 2018). Taken together, our results suggest that the interplay between diatom diversity and abundance is not merely additive, but a feedback loop modulated by external environmental conditions.

4.4 Diatom productivity and its possible role in the E/O cooling

Studies to date indicate that, across the EOT, SO regions experienced substantial shifts in productivity (e.g., Diester-Haass and Zahn, 1996; Diekmann et al., 2004; Anderson and Delaney, 2005; Egan et al., 2013; Villa et al., 2014; Plancq et al., 2014; Pascher et al., 2015; Rodrigues de Faria et al., 2024). These shifts **form the** basis for the hypothesis that increasing

productivity *contributed to* CO_2 drawdown through the biological carbon pump (Salamy and Zachos, 1999; Scher and Martin, 2006; Egan et al., 2013). Our results add weight to this view: records across the EOT show rising diatom accumulation together with increasing community diversity (Özen et al., subm.), consistent with Si isotope evidence for pulses of silica utilization and associated changes in carbon export (e.g., Egan et al., 2013). We emphasize, however, that diatom productivity was not an overriding mechanisms in itself but one element within a broader climatic and oceanographic mosaic that together shaped CO_2 drawdown across the E/O boundary.

A frequent **c**riticism of a diatom-driven increase in productivity and its potential role in E/O cooling is that opal-rich sediments are restricted to a few regions, such as the Agulhas Ridge and Falkland Plateau regions (e.g., Wade et al., 2020). However, this view largely reflects sediment classification systems that emphasize the most abundant component and have historically favored carbonate-rich deposits. Several biases contribute to the underrepresentation of biogenic silica in the deep-sea sediment record: (1) a bias towards carbonate pelagic sedimentation due to substantial carbonate rock weathering on land, (2) pelagic primary sediment names based on the most abundant single sedimentary component, and (3) a historical preference in deep-sea drilling for well-preserved carbonate sections, often chosen for geochemical studies. As a result, compilations which rely only on dominant sediment types, mostly reflect pelagic carbonates while underestimating the presence of biogenic silica. In contrast, studies using quantitative estimates of biogenic silica(e.g., smear slide analyses, Renaudie, 2016) provide a more accurate, though still incomplete, picture of silica accumulation. Given these limitations, the absence of opal-dominated sediments in broad sediment classifications does not contradict the evidence for increased biogenic opal deposition. Indeed, our results show a clear rise in biogenic opal across all targeted sites, providing robust evidence for enhanced diatom productivity across the EOT.

However, the mode and magnitude of the opal deposition/preservation vary between sites, reflecting local depositional settings and preservation conditions. Despite these differential geological filters, intervals of productivity reorganization identified in earlier studies are also evident in our records. Importantly, these productivity events coincide with taxonomic shifts in diatom communities (Özen et al., subm.), changes that may have tuned the efficiency of the biological carbon pump (Tréguer et al., 2018).

Diatoms are particularly effective exporters of organic carbon (Ragueneau et al., 2000; Tréguer et al., 2018). Diatom-dominated export buffers particulate organic carbon (POM) against microbial decomposition in the mesopelagic zone far more effectively than coccolithophore-dominated fluxes (e.g., Cabrera-Brufau et al., 2021). Thus, the late Eocene increase in diatom abundance and diversity would have improved the efficiency of the biological carbon pump, enhancing CO_2 drawdown even without a marked rise in total SO productivity. This effect gains further weight considering that the Eocene CO_2 levels were already close to threshold values (~750 ppm) thought necessary for Antarctic ice sheet initiation (DeConto and Pollard, 2003), though we note that such thresholds are model-dependent and vary with boundary conditions (Gasson et

al., 2014). Thus, increasing oceanic productivity and the greater efficiency of diatom-mediated carbon export may have provided *the final touch* that pushed CO_2 levels below the boundary conditions, contributing to the E/O climate shift.

5 Conclusion

475 This study focuses on the dynamics of diatom productivity and community diversity across the late Eocene, as the Cenozoic Hothouse came to an end and the SO underwent a major productivity reorganization form ~38 Ma onward. Our findings show a marked increase in diatom abundance alongside major reorganizations in both diatom (Özen et al., subm.) and radiolarian (Lazarus et al., 2008; Pascher et al., 2015) communities, consistent with an overall rise in SO productivity (e.g., Diester-Haass and Zahn, 1996; Anderson and Delaney, 2005; Villa et al., 2014; Rodrigues de Faria et al., 2024). These 480 changes point to a broad evolutionary and productivity shift, likely driven by major changes in ocean circulation, including the early development of the AMOC (e.g., Borrelli et al., 2014) and the strengthening of the circum-Antarctic currents (e.g., Houben et al., 2019; Sarkar et al., 2019; Rodrigues de Faria et al., 2024).

Bulk opal records are not fully informative for understanding diatom productivity and its impact on the biological carbon 485 pump and atmospheric CO_2. This is because bulk opal measurements (1) fail to differentiate between contributions from diatoms and other biosiliceous plankton, such as radiolarians and (2) overlook the biological background of productivity, particularly diversity and community composition, which is a critical component of diatom-mediated carbon sequestration (Tréguer et al., 2018). Our study integrates both the diversity and abundance dynamics of diatoms across the EOT, revealing that increases in both likely enhanced the efficiency of the biological carbon pump from 38 Ma onward. This enhancement 490 reflects not only higher diatom abundance but also more effective nutrient utilization linked to diversity, which together may have supported a stronger carbon flux to the ocean interior for a sustained period of time. We therefore highlight SO diatom expansion, through both abundance and diversity, as an important component of the late Eocene carbon cycling. While the precise strength of the link between diatoms and global cooling across the EOT remains uncertain, our results support the view that diatoms contributed to the efficiency of the biological carbon pump during this critical interval, and that their role 495 deserves continued attention in underestimating the mechanisms behind Cenozoic climate dynamics.

Data availability

The supplementary information and raw data are available in the Supplement, and the raw data will be available upon publication on Zenodo (10.5281/zenodo.14826336, Özen et al., 2025).

Supplement

500 The supplement related to this article is available online at:

Author Contribution

VÖ collected and analyzed the data and drafted the manuscript. All authors contributed to revision and editing of the final version.

Competing interests

505 The contact author has declared that none of the authors has any competing interests.

Acknowledgements

We thank Sylvia Dietze (MfN Berlin) for her assistance with sample preparation.

Financial Support

This study was funded by the Federal Ministry of Education and Research (BMBF) under the "Make our Planet Great Again
510 – German Research Initiative", grant number 57429681, implemented by the German Academic Exchange Service (DAAD).

References

Abrantes, F., Cermeño, P., Lopes, C., Romero, O., Matos, L., Van Iperen, J., Rufino, M., and Magalhães, V.: Diatoms Si Uptake Capacity Drives Carbon Export In Coastal Upwelling Systems, https://doi.org/10.5194/bg-2015-517, 22 February 2016.

515

Anagnostou, E., John, E. H., Babila, T. L., Sexton, P. F., Ridgwell, A., Lunt, D. J., Pearson, P. N., Chalk, T. B., Pancost, R. D., and Foster, G. L.: Proxy evidence for state-dependence of climate sensitivity in the Eocene greenhouse, Nature Communications, 11, 4436, https://doi.org/10.1038/s41467-020-17887-x, 2020.

520 Anderson, L. D. and Delaney, M. L.: Middle Eocene to early Oligocene paleoceanography from Agulhas Ridge, Southern Ocean (Ocean Drilling Program Leg 177, Site 1090): Eocene-Oligocene Paleoceanography, Paleoceanography, 20, https://doi.org/10.1029/2004PA001043, 2005.

Baldauf, J. G. and Barron, J. A.: Evolution of Biosiliceous Sedimentation Patterns Eocene Through Quaternary: Paleoceanographic Response to Polar Cooling, in: Geological History of the Polar Oceans: Arctic versus Antarctic, edited by: Bleil, U. and Thiede, J., Springer Netherlands, Dordrecht, 575–607, https://doi.org/10.1007/978-94-009-2029-3_32, 1990.

Barker, P. F.: Scotia Sea regional tectonic evolution: Implications for mantle flow and palaeocirculation, Earth-Science Reviews, 55, 1–39, https://doi.org/10.1016/s0012-8252(01)00055-1, 2001.

Barker, P. F., Filippelli, G. M., Florindo, F., Martin, E. E., and Scher, H. D.: Onset and role of the Antarctic Circumpolar Current, Deep Sea Research Part II: Topical Studies in Oceanography, 54, 2388–2398, https://doi.org/10.1016/j.dsr2.2007.07.028, 2007.

Barron, J. A., Stickley, C. E., and Bukry, D.: Paleoceanographic, and paleoclimatic constraints on the global Eocene diatom and silicoflagellate record, Palaeogeography, Palaeoclimatology, Palaeoecology, 422, 85–100, https://doi.org/10.1016/j.palaeo.2015.01.015, 2015.

Bohaty, S. M. and Zachos, J. C.: Significant Southern Ocean warming event in the late middle Eocene, Geology, 31, 1017–1020, https://doi.org/10.1130/G19800.1, 2003.

Borrelli, C., Cramer, B. S., and Katz, M. E.: Bipolar Atlantic deepwater circulation in the middle-late Eocene: Effects of Southern Ocean gateway openings, Paleoceanography, 29, 308–327, https://doi.org/10.1002/2012PA002444, 2014.

Bryłka, K., Witkowski, J., and Bohaty, S. M.: Biogenic silica accumulation and diatom assemblage variations through the Eocene-Oligocene Transition: A Southern Indian Ocean versus South Atlantic perspective, Palaeogeography, Palaeoclimatology, Palaeoecology, 636, 111971, https://doi.org/10.1016/j.palaeo.2023.111971, 2024.

Cabrera-Brufau, M., Arin, L., Sala, M. M., Cermeño, P., and Marrasé, C.: Diatom dominance enhances resistance of phytoplanktonic POM to mesopelagic microbial decomposition, Frontiers in Marine Science, 8, https://doi.org/10.3389/fmars.2021.683354, 2021.

Cortese, G., Gersonde, R., Hillenbrand, C.-D., and Kuhn, G.: Opal sedimentation shifts in the World Ocean over the last 15 Myr, Earth and Planetary Science Letters, 224, 509–527, https://doi.org/10.1016/j.epsl.2004.05.035, 2004.

Coxall, H. K. and Pearson, P. N.: The Eocene–Oligocene Transition, in: Deep-time perspectives on climate change: Marrying the signal from computer models and biological proxies, The Geological Society of London on behalf of The Micropalaeontological Society, 351–387, https://doi.org/10.1144/tms002.16, 2007.

560

Coxall, H. K., Wilson, P. A., Pälike, H., Lear, C. H., and Backman, J.: Rapid stepwise onset of Antarctic glaciation and deeper calcite compensation in the Pacific Ocean, Nature, 433, 53–57, https://doi.org/10.1038/nature03135, 2005.

DeConto, R. M. and Pollard, D.: Rapid Cenozoic glaciation of antarctica induced by declining atmospheric CO2, Nature,

565   421, 245–249, https://doi.org/10.1038/nature01290, 2003.

Diekmann, B., Kuhn, G., Gersonde, R., and Mackensen, A.: Middle Eocene to early Miocene environmental changes in the sub-Antarctic Southern Ocean: Evidence from biogenic and terrigenous depositional patterns at ODP site 1090, Global and Planetary Change, 40, 295–313, https://doi.org/10.1016/j.gloplacha.2003.09.001, 2004.

570

Diester-Haass, L. and Zahn, R.: Eocene-Oligocene transition in the Southern Ocean: History of water mass circulation and biological productivity, Geol, 24, 163, https://doi.org/10.1130/0091-7613(1996)024%253C0163:eotits%253E2.3.co;2, 1996.

Douglas, P. M. J., Affek, H. P., Ivany, L. C., Houben, A. J. P., Sijp, W. P., Sluijs, A., Schouten, S., and Pagani, M.:

575   Pronounced zonal heterogeneity in Eocene southern high-latitude sea surface temperatures, Proc. Natl. Acad. Sci. U.S.A., 111, 6582–6587, https://doi.org/10.1073/pnas.1321441111, 2014.

Egan, K. E., Rickaby, R. E. M., Hendry, K. R., and Halliday, A. N.: Opening the gateways for diatoms primes earth for Antarctic glaciation, Earth and Planetary Science Letters, 375, 34–43, https://doi.org/10.1016/j.epsl.2013.04.030, 2013.

580

Ehrmann, W. U.: Implications of sediment composition on the southern Kerguelen Plateau for paleoclimate and depositional environment, in: Proceedings of the ocean drilling program, 119 scientific results, Ocean Drilling Program, https://doi.org/10.2973/odp.proc.sr.119.121.1991, 1991.

585   Ehrmann, W. U. and Mackensen, A.: Sedimentological evidence for the formation of an east Antarctic ice sheet in Eocene/Oligocene time, Palaeogeography, Palaeoclimatology, Palaeoecology, 93, 85–112, https://doi.org/10.1016/0031-0182(92)90185-8, 1992.

Elsworth, G., Galbraith, E., Halverson, G., and Yang, S.: Enhanced weathering and CO2 drawdown caused by latest Eocene

590 strengthening of the Atlantic meridional overturning circulation, Nature Geoscience, 10, 213–216, https://doi.org/10.1038/ngeo2888, 2017.

Evangelinos, D., Escutia, C., Flierdt, T. van de, Valero, L., Flores, J.-A., Harwood, D. M., Hoem, F. S., Bijl, P., Etourneau, J., Kreissig, K., Nilsson-Kerr, K., Holder, L., López-Quirós, A., and Salabarnada, A.: Absence of a strong, deep-reaching

595 antarctic circumpolar current zonal flow across the Tasmanian gateway during the Oligocene to early Miocene, Global and Planetary Change, 208, 103718, https://doi.org/10.1016/j.gloplacha.2021.103718, 2022.

Evangelinos, D., Etourneau, J., Van De Flierdt, T., Crosta, X., Jeandel, C., Flores, J.-A., Harwood, D. M., Valero, L., Ducassou, E., Sauermilch, I., Klocker, A., Cacho, I., Pena, L. D., Kreissig, K., Benoit, M., Belhadj, M., Paredes, E., Garcia-

600 Solsona, E., López-Quirós, A., Salabarnada, A., and Escutia, C.: Late Miocene onset of the modern Antarctic Circumpolar Current, Nat. Geosci., https://doi.org/10.1038/s41561-023-01356-3, 2024.

Farmer, J. R., Hertzberg, J. E., Cardinal, D., Fietz, S., Hendry, K., Jaccard, S. L., Paytan, A., Rafter, P. A., Ren, H., Somes, C. J., Sutton, J. N., and GEOTRACES-PAGES Biological Productivity Working Group Members: Assessment of C, N and

605 Si isotopes as tracers of past ocean nutrient and carbon cycling, Global Biogeochem Cycles, https://doi.org/10.1029/2020GB006775, 2021.

Faul, K. L. and Delaney, M. L.: A comparison of early Paleogene export productivity and organic carbon burial flux for Maud Rise, Weddell Sea, and Kerguelen Plateau, south Indian Ocean, Paleoceanography, 25,

610 https://doi.org/10.1029/2009PA001916, 2010.

Funakawa, S. and Nishi, H.: Radiolarian faunal changes during the Eocene-Oligocene transition in the Southern Ocean (maud rise, ODP leg 113, site 689) and its significance in paleoceanographic change, Micropaleontology, 54, 15–26, https://doi.org/10.47894/mpal.54.1.03, 2008.

615

Gasson, E., Lunt, D. J., DeConto, R., Goldner, A., Heinemann, M., Huber, M., LeGrande, A. N., Pollard, D., Sagoo, N., Siddall, M., Winguth, A., and Valdes, P. J.: Uncertainties in the modelled CO2 threshold for Antarctic glaciation, Clim. Past, 10, 451–466, https://doi.org/10.5194/cp-10-451-2014, 2014.

620 Hatton, I. A., Mazzarisi, O., Altieri, A., and Smerlak, M.: Diversity begets stability: Sublinear growth and competitive coexistence across ecosystems, Science, 383, https://doi.org/10.1126/science.adg8488, 2024.

Hodel, F., Grespan, R., De Rafélis, M., Dera, G., Lezin, C., Nardin, E., Rouby, D., Aretz, M., Steinnman, M., Buatier, M., Lacan, F., Jeandel, C., and Chavagnac, V.: Drake Passage gateway opening and Antarctic Circumpolar Current onset 31 Ma ago: The message of foraminifera and reconsideration of the Neodymium isotope record, Chemical Geology, 570, 120171, https://doi.org/10.1016/j.chemgeo.2021.120171, 2021.

Hodel, F., Fériot, C., Dera, G., De Rafélis, M., Lezin, C., Nardin, E., Rouby, D., Aretz, M., Antonio, P., Buatier, M., Steinmann, M., Lacan, F., Jeandel, C., and Chavagnac, V.: Eocene-Oligocene southwest Pacific Ocean paleoceanography new insights from foraminifera chemistry (DSDP site 277, Campbell Plateau), Front. Earth Sci., 10, 998237, https://doi.org/10.3389/feart.2022.998237, 2022.

Houben, A. J. P., Bijl, P. K., Sluijs, A., Schouten, S., and Brinkhuis, H.: Late Eocene Southern Ocean Cooling and Invigoration of Circulation Preconditioned Antarctica for Full‐Scale Glaciation, Geochem Geophys Geosyst, 20, 2214–2234, https://doi.org/10.1029/2019GC008182, 2019.

Hutchinson, D. K., Coxall, H. K., Lunt, D. J., Steinthorsdottir, M., Boer, A. M. de, Baatsen, M., Heydt, A. von der, Huber, M., Kennedy-Asser, A. T., Kunzmann, L., Ladant, J.-B., Lear, C. H., Moraweck, K., Pearson, P. N., Piga, E., Pound, M. J., Salzmann, U., Scher, H. D., Sijp, W. P., Śliwińska, K. K., Wilson, P. A., and Zhang, Z.: The Eocene–oligocene transition: A review of marine and terrestrial proxy data, models and model–data comparisons, Climate of the Past, 17, 269–315, https://doi.org/10.5194/cp-17-269-2021, 2021.

Kennett, J. P.: Cenozoic evolution of Antarctic glaciation, the circum-Antarctic Ocean, and their impact on global paleoceanography, J. Geophys. Res., 82, 3843–3860, https://doi.org/10.1029/JC082i027p03843, 1977.

Klages, J. P., Hillenbrand, C.-D., Bohaty, S. M., Salzmann, U., Bickert, T., Lohmann, G., Knahl, H. S., Gierz, P., Niu, L., Titschack, J., Kuhn, G., Frederichs, T., Müller, J., Bauersachs, T., Larter, R. D., Hochmuth, K., Ehrmann, W., Nehrke, G., Rodríguez-Tovar, F. J., Schmiedl, G., Spezzaferri, S., Läufer, A., Lisker, F., Van De Flierdt, T., Eisenhauer, A., Uenzelmann-Neben, G., Esper, O., Smith, J. A., Pälike, H., Spiegel, C., Dziadek, R., Ronge, T. A., Freudenthal, T., and Gohl, K.: Ice sheet–free West Antarctica during peak early Oligocene glaciation, Science, 385, 322–327, https://doi.org/10.1126/science.adj3931, 2024.

Ladant, J.-B., Donnadieu, Y., and Dumas, C.: Links between CO_2, glaciation and water flow: Reconciling the Cenozoic history of the Antarctic circumpolar current, Climate of the Past, 10, 1957–1966, https://doi.org/10.5194/cp-10-1957-2014, 2014.

Lauretano, V., Kennedy-Asser, A. T., Korasidis, V. A., Wallace, M. W., Valdes, P. J., Lunt, D. J., Pancost, R. D., and Naafs, B. D. A.: Eocene to Oligocene terrestrial southern hemisphere cooling caused by declining pCO2, Nature Geoscience, 14, 659–664, https://doi.org/10.1038/s41561-021-00788-z, 2021.

660

Lazarus, D.: An improved cover-slip holder for preparing microslides of randomly distributed particles, Journal of Sedimentary Research, 64, 686–0, https://doi.org/10.2110/jsr.64.686, 1994.

Lazarus, D., Hollis, C. J., and Apel, M.: Patterns of opal and radiolarian change in the Antarctic mid-Paleogene: Clues to the

665 origin of the Southern Ocean, Micropaleontology, 54, 41–48, https://doi.org/10.47894/mpal.54.1.05, 2008.

Lazarus, D., Barron, J., Renaudie, J., Diver, P., and Türke, A.: Cenozoic planktonic marine diatom diversity and correlation to climate change, PLoS ONE, 9, e84857, https://doi.org/10.1371/journal.pone.0084857, 2014.

670 Lear, C. H., Bailey, T. R., Pearson, P. N., Coxall, H. K., and Rosenthal, Y.: Cooling and ice growth across the Eocene-Oligocene transition, Geology, 36, 251–254, https://doi.org/10.1130/G24584A.1, 2008.

Liu, Z., Pagani, M., Zinniker, D., DeConto, R., Huber, M., Brinkhuis, H., Shah, S. R., Leckie, R. M., and Pearson, A.: Global Cooling During the Eocene-Oligocene Climate Transition, Science, 323, 1187–1190,

675 https://doi.org/10.1126/science.1166368, 2009.

Livermore, R., Hillenbrand, C., Meredith, M., and Eagles, G.: Drake passage and Cenozoic climate: An open and shut case?, Geochemistry, Geophysics, Geosystems, 8, https://doi.org/10.1029/2005gc001224, 2007.

680 Mackensen, A.: Changing Southern Ocean palaeocirculation and effects on global climate, Antarctic Science, 16, 369–386, https://doi.org/10.1017/s0954102004002202, 2004.

Malviya, S., Scalco, E., Audic, S., Vincent, F., Veluchamy, A., Poulain, J., Wincker, P., Iudicone, D., De Vargas, C., Bittner, L., Zingone, A., and Bowler, C.: Insights into global diatom distribution and diversity in the world's ocean, Proc. Natl. Acad.

685 Sci. U.S.A., 113, https://doi.org/10.1073/pnas.1509523113, 2016.

Mittelbach, G. G., Scheiner, S. M., and Steiner, C. F.: What Is the Observed Relationship Between Species Richness and Productivity? Reply, Ecology, 84, 3390–3395, https://doi.org/10.1890/03-3077, 2003.

690 Müller, R. D., Cannon, J., Qin, X., Watson, R. J., Gurnis, M., Williams, S., Pfaffelmoser, T., Seton, M., Russell, S. H. J., and Zahirovic, S.: GPlates: Building a Virtual Earth Through Deep Time, Geochem. Geophy. Geosy., 19, 2243–2261, https://doi.org/10.1029/2018GC007584, 2018

Nilsen, E. B., Anderson, L. D., and Delaney, M. L.: Paleoproductivity, nutrient burial, climate change and the carbon cycle

695 in the western equatorial Atlantic across the Eocene/Oligocene boundary: EOCENE/OLIGOCENE PRODUCTIVITY, Paleoceanography, 18, n/a-n/a, https://doi.org/10.1029/2002PA000804, 2003.

Özen, V., Renaudie, J., and Lazarus, D.: Unraveling Southern Ocean Diatom Diversity Across the Eocene/Oligocene Transition, the Journal of Micropalaeontology, subm.

700

Özen, V., Lazarus, D., Renaudie, J., & Faria, G.: Increasing opal productivity in the Late Eocene Southern Ocean: Evidence for increased carbon export preceding the Eocene-Oligocene glaciation [Data set]. Zenodo. https://doi.org/10.5281/zenodo.14826336, 2025

705 Pascher, K. M., Hollis, C. J., Bohaty, S. M., Cortese, G., McKay, R. M., Seebeck, H., Suzuki, N., and Chiba, K.: Expansion and diversification of high-latitude radiolarian assemblages in the late Eocene linked to a cooling event in the southwest Pacific, Clim. Past, 11, 1599–1620, https://doi.org/10.5194/cp-11-1599-2015, 2015.

Paxman, G. J. G., Jamieson, S. S. R., Hochmuth, K., Gohl, K., Bentley, M. J., Leitchenkov, G., and Ferraccioli, F.:

710 Reconstructions of Antarctic topography since the Eocene–Oligocene boundary, Palaeogeography, Palaeoclimatology, Palaeoecology, 535, 109346, https://doi.org/10.1016/j.palaeo.2019.109346, 2019.

Plancq, J., Mattioli, E., Pittet, B., Simon, L., and Grossi, V.: Productivity and sea-surface temperature changes recorded during the late Eocene early Oligocene at DSDP Site 511 (South Atlantic), Palaeogeography, Palaeoclimatology,

715 Palaeoecology, 407, 34–44, https://doi.org/10.1016/j.palaeo.2014.04.016, 2014.

R. Rintoul, S., W. Hughes, C., and Olbers, D.: Chapter 4.6 The antarctic circumpolar current system, in: International Geophysics, vol. 77, Elsevier, 271–XXXVI, https://doi.org/10.1016/S0074-6142(01)80124-8, 2001.

720 Rabosky, D. L. and Sorhannus, U.: Diversity dynamics of marine planktonic diatoms across the Cenozoic, Nature, 457, 183–186, https://doi.org/10.1038/nature07435, 2009.

Ragueneau, O., Tréguer, P., Leynaert, A., Anderson, R. F., Brzezinski, M. A., DeMaster, D. J., Dugdale, R. C., Dymond, J., Fischer, G., François, R., Heinze, C., Maier-Reimer, E., Martin-Jézéquel, V., Nelson, D. M., and Quéguiner, B.: A review of

725 the Si cycle in the modern ocean: Recent progress and missing gaps in the application of biogenic opal as a paleoproductivity proxy, Global and Planetary Change, 26, 317–365, https://doi.org/10.1016/S0921-8181(00)00052-7, 2000.

Ragueneau, O., Schultes, S., Bidle, K., Claquin, P., and Moriceau, B.: Si and C interactions in the world ocean: Importance of ecological processes and implications for the role of diatoms in the biological pump: Si AND C INTERACTIONS IN

730 THE OCEAN, Global Biogeochem. Cycles, 20, https://doi.org/10.1029/2006GB002688, 2006.

Renaudie, J.: Quantifying the Cenozoic marine diatom deposition history: Links to the C and Si cycles, Biogeosciences, 13, 6003–6014, https://doi.org/10.5194/bg-13-6003-2016, 2016.

735 Renaudie, J., Lazarus, D., and Diver, P.: NSB (Neptune Sandbox Berlin): An expanded and improved database of marine planktonic microfossil data and deep-sea stratigraphy, Palaeontologia Electronica, https://doi.org/10.26879/1032, 2020.

Renaudie, J., Lazarus, D., and Diver, P.: Archive of Neptune (NSB) database backups, https://doi.org/10.5281/ZENODO.10063218, 2023.

740
Robert, C., Diester-Haass, L., and Chamley, H.: Late Eocene–Oligocene oceanographic development at southern high latitudes, from terrigenous and biogenic particles: A comparison of Kerguelen Plateau and Maud Rise, ODP Sites 744 and 689, Marine Geology, 191, 37–54, https://doi.org/10.1016/S0025-3227(02)00508-X, 2002.

745 Rodrigues de Faria, G., Lazarus, D., Renaudie, J., Stammeier, J., Özen, V., and Struck, U.: Late eocene to early oligocene productivity events in the proto-Southern Ocean and correlation to climate change, Climate of the Past, 20, 1327–1348, https://doi.org/10.5194/cp-20-1327-2024, 2024.

Salamy, K. A. and Zachos, J. C.: Latest Eocene-Early Oligocene climate change and Southern Ocean fertility: Inferences

750 from sediment accumulation and stable isotope data, Palaeogeography, Palaeoclimatology, Palaeoecology, 145, 61–77, https://doi.org/10.1016/S0031-0182(98)00093-5, 1999.

Sarkar, S., Basak, C., Frank, M., Berndt, C., Huuse, M., Badhani, S., and Bialas, J.: Late Eocene onset of the Proto-Antarctic Circumpolar Current, Sci Rep, 9, 10125, https://doi.org/10.1038/s41598-019-46253-1, 2019.

755

Sauermilch, I., Whittaker, J. M., Klocker, A., Munday, D. R., Hochmuth, K., Bijl, P. K., and LaCasce, J. H.: Gateway-driven weakening of ocean gyres leads to Southern Ocean cooling, Nat Commun, 12, https://doi.org/10.1038/s41467-021-26658-1, 2021.

760 Scher, H. D. and Martin, E. E.: Timing and Climatic Consequences of the Opening of Drake Passage, Science, 312, 428–430, https://doi.org/10.1126/science.1120044, 2006.

Scher, H. D., Bohaty, S. M., Zachos, J. C., and Delaney, M. L.: Two-stepping into the icehouse: East Antarctic weathering during progressive ice-sheet expansion at the Eocene-Oligocene transition, Geology, 39, 383–386, 765 https://doi.org/10.1130/G31726.1, 2011.

Scher, H. D., Bohaty, S. M., Smith, B. W., and Munn, G. H.: Isotopic interrogation of a suspected late Eocene glaciation: Hidden glaciation revealed in the Eocene, Paleoceanography, 29, 628–644, https://doi.org/10.1002/2014pa002648, 2014.

770 Schumacher, S. and Lazarus, D.: Regional differences in pelagic productivity in the late Eocene to early Oligocene comparison of southern high latitudes and lower latitudes, Palaeogeography, Palaeoclimatology, Palaeoecology, 214, 243–263, https://doi.org/10.1016/S0031-0182(04)00424-9, 2004.

Shackleton, N. J. and Kennett, J. P.: Paleotemperature history of the Cenozoic and the initiation of Antarctic glaciation: 775 Oxygen and carbon isotope analyses in DSDP sites 277, 279 and 281, in: Initial reports of the deep-sea drilling project, 29, U.S. Government Printing Office, https://doi.org/10.2973/dsdp.proc.29.117.1975, 1975.

Shipboard Scientific Party: Site 511. In: Initial Reports of the Deep-Sea Drilling Project, edited by Ludwig, W. J., Krasheninnikov, V. A. et al., 71: Washington (U.S. Govt. Printing Office). 1983.
780
Shipboard Scientific Party: Site 689. In: Proceedings of the Ocean Drilling Program, Initial Reports, edited by Barker, P. R, Kennett, J. P., et al, 113: College Station, TX (Ocean Drilling Program). 1988.

Shipboard Scientific Party: Site 748. In: Proceedings of the Ocean Drilling Program, Initial Reports, edited by Schlich, R., 785 Wise, S. W., Jr., et al., 120: College Station, TX (Ocean Drilling Program) 1989.

Shipboard Scientific Party: Site 1090. In: Proceedings of the Ocean Drilling Program, Initial Reports edited by Gersonde, R., Hodell, D.A., Blum, P., et al., 177: College Station, TX (Ocean Drilling Program) 1998.

790 Stickley, C. E., Brinkhuis, H., Schellenberg, S. A., Sluijs, A., Röhl, U., Fuller, M., Grauert, M., Huber, M., Warnaar, J., and Williams, G. L.: Timing and nature of the deepening of the Tasmanian Gateway, Paleoceanography, 19, 2004PA001022, https://doi.org/10.1029/2004PA001022, 2004.

Stickley, C. E., Brinkhuis, H., Schellenberg, S. A., Sluijs, A., Röhl, U., Fuller, M., Grauert, M., Huber, M., Warnaar, J., and 795 Williams, G. L.: Timing and nature of the deepening of the Tasmanian Gateway: Deepening of the Tasmanian Gateway, Paleoceanography, 19, n/a-n/a, https://doi.org/10.1029/2004PA001022, 2004.

Straume, E. O., Nummelin, A., Gaina, C., and Nisancioglu, K. H.: Climate transition at the Eocene Oligocene influenced by bathymetric changes to the Atlantic Arctic oceanic gateways, Proceedings of the National Academy of Sciences, 119, 800 e2115346119, https://doi.org/10.1073/pnas.2115346119, 2022.

Ted C. Moore: Method of randomly distributing grains for microscopic examination, J. Sediment. Res., 43, https://doi.org/10.1306/74d728ba-2b21-11d7-8648000102c1865d, 1973.

805 Toumoulin, A., Donnadieu, Y., Ladant, J.-B., Batenburg, S. J., Poblete, F., and Dupont-Nivet, G.: Quantifying the Effect of the Drake Passage Opening on the Eocene Ocean, Paleoceanography and Paleoclimatology, 35, e2020PA003889, https://doi.org/10.1029/2020PA003889, 2020.

Tréguer, P., Nelson, D. M., Van Bennekom, A. J., DeMaster, D. J., Leynaert, A., and Quéguiner, B.: The silica balance in 810 the world ocean: A reestimate, Science, 268, 375–379, https://doi.org/10.1126/science.268.5209.375, 1995.

Tréguer, P., Bowler, C., Moriceau, B., Dutkiewicz, S., Gehlen, M., Aumont, O., Bittner, L., Dugdale, R., Finkel, Z., Iudicone, D., Jahn, O., Guidi, L., Lasbleiz, M., Leblanc, K., Levy, M., and Pondaven, P.: Influence of diatom diversity on the ocean biological carbon pump, Nature Geoscience, 11, 27–37, https://doi.org/10.1038/s41561-017-0028-x, 2018.

815

Villa, G., Fioroni, C., Pea, L., Bohaty, S., and Persico, D.: Middle Eocene–late Oligocene climate variability: Calcareous nannofossil response at Kerguelen Plateau, Site 748, Marine Micropaleontology, 69, 173–192, https://doi.org/10.1016/j.marmicro.2008.07.006, 2008.

820 Villa, G., Fioroni, C., Persico, D., Roberts, A. P., and Florindo, F.: Middle Eocene to Late Oligocene Antarctic glaciation/deglaciation and Southern Ocean productivity, Paleoceanography, 29, 223–237, https://doi.org/10.1002/2013PA002518, 2014.

Virta, L., Gammal, J., Järnström, M., Bernard, G., Soininen, J., Norkko, J., and Norkko, A.: The diversity of benthic diatoms affects ecosystem productivity in heterogeneous coastal environments, Ecology, 100, e02765, https://doi.org/10.1002/ecy.2765, 2019.

Wade, B. S., O'Neill, J. F., Phujareanchaiwon, C., Ali, I., Lyle, M., and Witkowski, J.: Evolution of deep-sea sediments across the Paleocene-Eocene and Eocene-Oligocene boundaries, Earth-Science Reviews, 211, 103403, https://doi.org/10.1016/j.earscirev.2020.103403, 2020.

Westacott, S., Planavsky, N. J., Zhao, M.-Y., and Hull, P. M.: Revisiting the sedimentary record of the rise of diatoms, Proceedings of the National Academy of Sciences, 118, https://doi.org/10.1073/pnas.2103517118, 2021.

Westerhold, T., Marwan, N., Drury, A. J., Liebrand, D., Agnini, C., Anagnostou, E., Barnet, J. S. K., Bohaty, S. M., De Vleeschouwer, D., Florindo, F., Frederichs, T., Hodell, D. A., Holbourn, A. E., Kroon, D., Lauretano, V., Littler, K., Lourens, L. J., Lyle, M., Pälike, H., Röhl, U., Tian, J., Wilkens, R. H., Wilson, P. A., and Zachos, J. C.: An astronomically dated record of Earth's climate and its predictability over the last 66 million years, Science, 369, 1383–1387, https://doi.org/10.1126/science.aba6853, 2020.

Wilson, D. S. and Luyendyk, B. P.: West Antarctic paleotopography estimated at the Eocene☐Oligocene climate transition, Geophysical Research Letters, 36, https://doi.org/10.1029/2009gl039297, 2009.

Wilson, D. S., Pollard, D., DeConto, R. M., Jamieson, S. S. R., and Luyendyk, B. P.: Initiation of the West Antarctic Ice Sheet and estimates of total Antarctic ice volume in the earliest Oligocene, Geophysical Research Letters, 40, 4305–4309, https://doi.org/10.1002/grl.50797, 2013.

Witkowski, J., Bohaty, S. M., McCartney, K., and Harwood, D. M.: Enhanced siliceous plankton productivity in response to middle Eocene warming at Southern Ocean ODP Sites 748 and 749, Palaeogeography, Palaeoclimatology, Palaeoecology, 326–328, 78–94, https://doi.org/10.1016/j.palaeo.2012.02.006, 2012.

Witkowski, J., Bryłka, K., Bohaty, S. M., Mydłowska, E., Penman, D. E., and Wade, B. S.: North Atlantic marine biogenic silica accumulation through the early to middle Paleogene: Implications for ocean circulation and silicate weathering feedback, Climate of the Past, 17, 1937–1954, https://doi.org/10.5194/cp-17-1937-2021, 2021.

Zachos, J. and Kump, L.: Carbon cycle feedbacks and the initiation of Antarctic glaciation in the earliest Oligocene, Global and Planetary Change, 47, 51–66, https://doi.org/10.1016/j.gloplacha.2005.01.001, 2005.

Zachos, J., Pagani, M., Sloan, L., Thomas, E., and Billups, K.: Trends, rhythms, and aberrations in global climate 65 Ma to
860 present, Science, 292, 686–693, https://doi.org/10.1126/science.1059412, 2001.

Zachos, J. C., Quinn, T. M., and Salamy, K. A.: High☐resolution (104 years) deep☐sea foraminiferal stable isotope records
of the Eocene-Oligocene climate transition, Paleoceanography, 11, 251–266, https://doi.org/10.1029/96pa00571, 1996.

865 Zhang, Y. G., Pagani, M., Liu, Z., Bohaty, S. M., and DeConto, R.: A 40-million-year history of atmospheric CO2,
Philosophical Transactions of the Royal Society A: Mathematical, Physical and Engineering Sciences, 371, 20130096,
https://doi.org/10.1098/rsta.2013.0096, 2013.